* Title page with author details

Electrical discharge milling with oblong tools

I.J. Mikesic, R.V. Fleisig, P. Koshy *

Department of Mechanical Engineering, McMaster University, Hamilton, Canada

Abstract

Electrical discharge milling is an emerging technology which entails a rotating cylindrical tool that is traversed along a predefined tool path to machine a cavity. This process configuration offers advantages such as minimal time/cost associated with tool manufacture and improved gap flushing, as compared to traditional die-sinking that involves complex three-dimensional tools. Rotating cylindrical tools however inherently preclude the machining of sharp features and correspond to increased relative electrode wear; the reduced machining engagement further restricts the machining power which in turn limits the removal rate. To this end, this paper presents a novel tooling concept that relates to a set of standard prismatic tools of an oblong section, which incorporate the favorable functional characteristics of both electrical discharge milling and die-sinking technologies. Aspects of computer-aided manufacture referring to tool selection, sizing and path planning are discussed. The concepts developed are illustrated through the application of an oblong tool that rotates and translates to machine a sample two-dimensional cavity.

Key words: computer-aided manufacture, electrical discharge machining, novel tooling, spark erosion, tool path planning

* Corresponding author
Email address: koshy@mcmaster.ca (P. Koshy).

Electrical discharge milling with oblong tools

Abstract

Electrical discharge milling is an emerging technology which entails a rotating cylindrical tool that is traversed along a predefined tool path to machine a cavity. This process configuration offers advantages such as minimal time/cost associated with tool manufacture and improved gap flushing, as compared to traditional die-sinking that involves complex three-dimensional tools. Rotating cylindrical tools however inherently preclude the machining of sharp features and correspond to increased relative electrode wear; the reduced machining engagement further restricts the machining power which in turn limits the removal rate. To this end, this paper presents a novel tooling concept that relates to a set of standard prismatic tools of an oblong section, which incorporate the favorable functional characteristics of both electrical discharge milling and die-sinking technologies. Aspects of computer-aided manufacture referring to tool selection, sizing and path planning are discussed. The concepts developed are illustrated through the application of an oblong tool that rotates and translates to machine a sample two-dimensional cavity.

Key words: computer-aided manufacture, electrical discharge machining, novel tooling, spark erosion, tool path planning

1 Introduction

First-generation ram (sinker) EDM machine tools comprised a single servo-controlled axis to plunge feed a tool of a shape complementary to that required in the workpiece. The primary limitations of this technology are the time and cost associated with fabricating complex tools; particularly that depending on the tolerances required and tool wear, the process necessitates several tools to sequentially approach the desired workpiece geometry. There are issues with effective flushing of the machining gap as well, especially for applications with deep features and/or a large frontal machining area, which renders the process unstable, reduces the removal rate and adversely affects the integrity of the machined surface. Techniques such as jump-EDM have been successfully implemented to improve flushing in such instances, but at the expense of the periodic tool retraction off the gap representing lost machining time.

The introduction of computer numerical control (CNC) in EDM machine tools in the 1980s enabled novel machining strategies such as planetary/orbital EDM [1,2] that enhanced its capability profile. One of the first attempts to exploit CNC capabilities in EDM towards establishing it as a mainstream manufacturing process seems to be due to Saito et al. who proposed [3] the concept of traversing simple frame tools to machine cavities. This was eventually advanced further by Bayramoglu and Duffill to include cylindrical [4] and plate [5] tools. At the present time, ram EDM machine tools have evolved [6] to include four servo-controlled axes to realize electrical discharge milling (ED-milling), wherein a complex three-dimensional workpiece is machined layer-by-layer, by traversing a rotating solid cylindrical or tubular tool along a predefined tool path, resembling an end-milling operation.

The advantages of ED-milling include: (i) the minimal time and cost of tool manufacture as they refer to standard stock, and (ii) adequate flushing of the machining gap brought about by the relative motion between the tool and the workpiece, and the possibility of employing auxiliary jet flushing. The issue with ED-milling is that tool wear has an unfavorable influence on machining accuracy. This has been addressed to a large extent by resorting to intermittent tool redressing, and real-time tool wear sensing and compensation strategies [7]. Of particular note is the uniform wear method [8] wherein the tool path is specifically formulated to regain the tool shape at regular intervals, by reducing the three-dimensional tool wear to linear wear. ED-milling is particularly attractive for micromachining applications due to the non-contact nature of the EDM process that CAD/CAM systems have been specifically adapted [9] for this purpose.

The application of rotating tools in ED-milling entails the advantages of excellent flushing and even distribution of wear over the working surface of the tool; however, rotating tools inherently preclude the machining of pockets with sharp features. Corners could be generated with rotating tools of an appropriately small radius, but their application is not productive as the limited engagement restricts the maximum machining power, and thus limits the removal rate. Tools of a small diameter are further prone to accelerated wear. To this end, a novel application inspired by the kinematics of a Reuleaux Triangle that uses rotating curvilinear tools has recently been developed [10] for sinking regular and non-regular polygonal shapes with sharp corners, so as to facilitate gap flushing while concurrently maximizing the frontal machining area. The work presented in the present paper expands on this concept, by proposing the application of innovative prismatic tools with an oblong cross-section that rotate and translate to machine a cavity.

The motivation for this work follows from the observation [2,5,11–13] that the material removal rate in EDM is maximized when operating at the optimal current per unit frontal machining area of the tool, provided adequate flushing of the machining gap is maintained; the use of a tool with a larger frontal area moreover corresponds [5] to a lower relative electrode wear (Fig. 1). To this end, this paper reports on aspects of a set of standardized tools that have been conceived expressly to: (i) entail minimal electrode manufacturing cost and time, (ii) maximize frontal machining area, (iii) facilitate good flushing, and (iv) be able to machine two-dimensional cavities with sharp corners. A summary of the functional characteristics of the proposed tool set vis-à-vis three-dimensional and cylindrical tools is presented in Table 1, wherein it can be seen that oblong tools combine the benefits of the other two configurations. This paper presents details pertaining to tool type selection, tool sizing, and path planning. An example is also provided to illustrate the various concepts developed.

2 Profile types and tool type selection

Cavities considered in this work entail single or multiple two-dimensional closed loop profiles, the latter corresponding to the presence of islands in the cavity. Segments that constitute the profile representing the cavity boundary are assumed to be G^2 (curvature) continuous. The profiles include round and/or sharp features, and are classified with reference to their geometric composition and continuity along concave regions (segments that open away from the interior of the cavity). Convexity is not considered in profile definition.

Fig. 2 shows the three profile types and the corresponding tools of length L, width W and centerline length L_c that are used to machine them. Type 1 profiles consist of concave regions in which all junctions are at least G^1 continuous (neighboring segments are tangent continuous at endpoints). Type 2 refers to profiles wherein all concave regions are G^0 continuous (neighboring segments are connected at their endpoints but are tangent discontinuous) and comprise only linear segments. Type 3 profiles consist of concave regions that include both linear and non-linear segments, with at least one concave region in which all junctions are G^0 continuous.

Tool selection is based on the geometric similarity between the types of profiles and tools; for instance, tool type 1 is G^1 continuous and therefore used for machining profile type 1, and so forth. Tool type 2 can be used to machine all profile types, however this may not maximize the frontal machining area.

3 Calculation of tool size

The tool types indicated in Fig. 2 are specified by their length L and width W. This section details the calculation of their maximum possible values with the aid of the Medial Axis Transform (MAT). MAT is a geometric representation that uses circles as primitives to reduce a profile into its medial axis and the associated radius function. The medial axis is the set of points defined by the centers of maximum inscribed circles (Fig. 3 shows just a few circles) that collectively represent the profile. The radius function is a continuous function that denotes the radii of the circles centered on the medial axis. Further information on MAT can be found in [14–18]; an algorithm outlined in [18] was used in this work to compute the MAT.

3.1 Calculation of tool width W

Tool width calculation is dependent on profile type and is presented accordingly. The maximum tool width is determined by the feature of minimum size in the profile to ensure accessibility of cavity features while machining, considering that the entire cavity is machined using a single tool. The feature of minimum size is defined as the smallest internal radius, the length of the shortest line in the profile, or the width of the narrowest channel if any.

Type 1 profiles are G^1 continuous with no sharp features, and hence the tool width may be calculated by simply searching the radius function for the minimum to detect the smallest internal radius or the width of a narrow channel. The maximum tool width is twice the minimum radius.

As type 2 profiles involve sharp features, the medial axis entails branches with radius functions approaching zero towards the corners (Fig. 4a). Searching the radius function for the minimum is therefore not practicable, and it is hence necessary to remove such branches (Fig. 4b). The smallest remaining radius is then compared against the feature of minimum length, determined by searching for the shortest line segment in the profile.

In profiles that involve tapered or convex segments, a direct search for the feature of minimum length will not return the appropriate value. Therefore, before the search is performed some lines must be discarded as per the following criteria: (1) if a line connects two linear segments and is not perpendicular to either, those segments that are shorter than the connecting line are eliminated; (2) moving in the counter-clockwise direction as a matter of convention, if a line is to the right of the segment before it, the line is eliminated; furthermore, if the segment before the line is linear, that is eliminated as well. Criterion 1 ensures that the search yields the connecting line in the presence of a taper (Fig. 5a), which represents the smallest width across the taper that limits the tool width. Criterion 2 removes lines that lie on convex regions of the profile (Fig. 5b) that may be traced by a tool of a larger width. The profile is now searched for the feature of minimum length for comparison against the tool width defined by the smallest value in the radius function. The smaller of the two values specifies the maximum permissible tool width.

Type 3 profiles combine elements of types 1 and 2, and hence the methods outlined above can be used to compute the tool width. Unlike type 2 profiles, type 3 profiles may contain concave regions that are G^1 continuous, but these regions are identified during the computation of the modified MAT.

3.2 Calculation of tool length L

On having calculated the tool width W, the next step is to determine the tool length L that maximizes the frontal machining area. For all tool types, the profile is offset by $W/2$ to first calculate the tool center line length L_c. The exact length L may be obtained thereafter for each tool type, as discussed at the end of this section.

Three different approaches are used for calculating L_c. The first approach entails the maximum inscribed circle (MIC) of the offset profile, obtained by searching the radius function of the offset profile for the maximum. Fig. 6 shows the MIC of an offset profile and the corresponding center line of length $2R$, where R is the radius of the MIC.

A tool length greater than that specified by the MIC is possible when a cavity comprises long narrow regions (as in Fig. 4 for example). The second method applies in such instances for concave regions of profile types 1 and 2; all convex regions of the offset profile are hence discarded during this search. In this method, the tool length is determined based on line segments in the profile offset. For such a line to be a solution, it should be able to reach all linear regions of the profile offset through either point or line contact. Beginning with the longest line on the profile offset, each line is therefore successively tested in the order of decreasing length for both point and line contact against all other segments on the offset profile.

In order for a line to make line contact with another segment, the segment must be a line and be longer than the line that it is tested against. As for point contact, the line in consideration is placed at the endpoint of the segment it is being tested against without intersecting the profile offset, such that it subtends the largest possible interior angle. If the interior angle is greater than $90°$ (Fig. 7a), the other endpoint of the line in consideration is connected to the furthest endpoint of the segment against which it is tested. This procedure is performed from both sides of the segment. When the angle formed between the segment and the line is less than $90°$ (Fig. 7b) the center line is constructed on the segment from the point at which it is normal to it. The endpoints of the line and those of the segment are joined to identify the bounded region that the tool can sweep. If the regions bounded by these lines (Figs. 7a & 7b) do not intersect the offset profile, the line in consideration can fully access the entire segment by point contact. In the order of decreasing length, the first line in the profile offset that can satisfy these conditions is chosen to define the tool center line length. The larger of this value and that referring to the MIC corresponds to the maximum possible tool center line length.

The third method applies to convex regions of the offset profile. For convex regions that are G^1 continuous (Fig. 8a), tangents constructed along the profile offset are used to determine the center line length. For the convex region in consideration, starting with the parameter $u = 0$, tangents are constructed incrementally both to the left and to the right of the point defined by u. This process is terminated at $u = 1$ and the sum of the tangent lengths is then searched for the minimum, which corresponds to the center line length L_c of the longest tool that can fit in the convex region. When a convex region is G^0 continuous (Fig. 8b), an angular bisector is constructed between the curves that make up the convexity. The direction vectors perpendicular to the bisector lines are extended both to the left and right of the profile offset to represent L_c described by this region. Once the values have been calculated for convex regions of the cavity, the minimum value is chosen. This value is then compared to values determined by the concave regions of the cavity. The smallest of these represents the largest possible L_c for the computed tool width W.

The exact tool length L for tool types 1 to 3 can now be calculated respectively as:

$$L_1 = L_c + W \tag{1}$$
$$L_2 = \sqrt{\rho^2 - W^2} \tag{2}$$
$$L_3 = (\sqrt{\rho^2 - W^2} + \rho)/2 \tag{3}$$

where $\rho = L_c + W$.

4 Tool path planning

Tool path planning strategies for machining two-dimensional pockets with cylindrical tools is presently well developed as documented in [19]. Relevant work pertaining to oblong tools is relatively scant and is due to Tang et al. who reported [20] on the area swept by a polygon undergoing just translation, Sambandan et al. who also considered [21] rotation, and the application of these approaches to planar mechanisms [22]. Tool paths developed in the present work refer to a 4-axis ram EDM, wherein the orientation of the tool (C) about the Z-axis can be controlled simultaneous to its translation along

X, Y and Z axes. Machining into the depth of the cavity (Z) is realized in an alternating layer-by-layer fashion that promotes machining by the frontal face of the tool. This approach also allows for the tool to be constantly engaged in machining without having to be retracted off the gap.

Before a 2D tool path is developed, the number of passes required to complete a single layer is to be determined. When the tool tip is tracing a profile it attempts to remain normal to it to maximize the swept area. Regions that are not swept by the tool can therefore be identified by offsetting the profile by a distance equal to the selected tool length L, and examining the direction of the offset segments in any closed loops formed. If they point towards the inside of the loop, the profile will not be machined in a single pass. Fig. 9a shows such an instance (the shaded region in the middle is not machined), while the same profile can be machined in a single pass using a longer tool (Fig. 9b) wherein the direction of the offset segments point away from the closed loop.

In general, the tool remains normal to the profile that it generates. Changes to tool orientation occur at critical points along the profile wherein the tool either ceases to remain normal to the profile with a view to not overcut the profile, or is rendered normal to it as it no longer oversteps the profile. Critical points are specified by the intersection of the tool length offset with the profile (see Fig. 10 to follow). Upon determining the number of passes per layer and the critical points, the tool path is planned according to the profile type. A cutter location (CL) data file is then generated to define the tool path in x, y and c coordinates. A post-processor is thereafter used to generate the G-code to machine the cavity to the required depth in an alternating to-and-fro, layer-by-layer fashion.

As type 1 profiles and tools are tangent continuous, an offset approach can be used to develop the associated tool paths. Upon offsetting the profile and any loops requiring multiple passes, the tool is driven along the profile segment-by-segment in the counter-clockwise direction, such that the center of the arc that constitutes one of the tool ends is constrained to be on the profile offset. In between, and in the absence of critical points, the tool orientation is maintained as normal as possible to the profile, to ensure maximum sweep of the tool. As the tool center is driven along the offset profile, tool orientation is calculated incrementally at critical points to avoid overcutting. In Fig. 10, the tool can be seen to lose its normal orientation at the critical point (position of the tool shown shaded), but remains as normal as possible to the profile for the remainder of segment; if the tool were to travel in a direction opposite to that indicated, it would regain its normal orientation at the critical point and maintain it until the next critical point.

Type 2 profiles include sharp corners, and therefore an offset approach does not suffice. In this case, the tool begins by being normal to the profile such that its width lies entirely on the profile. It is then traversed along the profile, segment-by-segment in the counter-clockwise direction, such that at least one point on the edge tracing the profile is constrained to be on it, to enable machining of the entire profile. When the tool is normal to the profile, both end points lay on it; however, at critical points where tool orientation changes, only one point may remain on the profile, as seen in Fig. 11(a) that shows several successive positions of the tool. When machining a sharp corner the end points on the tools tracing edge will be on different segments (Fig. 11b): the leading point moves from (2) to (3) as the trailing point moves from (1) to (2), such that the tool does not overcut the profile.

Tools used to machine type 3 profiles contain both round and square ends. To fully utilize the tool, it must therefore be capable of rotating 180° without retracting from the cavity, and hence the reason that the tool center line length must be less than or equal to the diameter of the MIC. To take advantage of the tool path planning strategies developed for the other profile types, two representations of the type 3 profile are required. The first one is the unmodified profile (Fig. 12a), which is machined by the square end of the tool. The second representation of the profile is obtained by constructing fillets of a radius equal to half the tool width at any interior sharp corners such that the profile is of type 1 (Fig. 12b).

To start with, the center of the rounded end of the tool is constrained to the profile offset at the point where the MIC intersects the offset. This allows the tool to rotate 180° at the end of each layer. From the starting point mentioned above, the round end of the tool is driven in the counter-clockwise direction, along the offset of the profile type 1 representation. The tool path planning method outlined for profiles of type 1 is utilized with a minor modification: as the other end of the tool is square, the tool orientation is calculated such that the sweeping edge of the tool does not intersect the profile.

Once the tool has returned to its starting position, it is rotated 180° such that the square end of the tool now lies on the profile. The approach used for the square end of the tool is similar to that of profile type 2. In some instances the square end of the tool may not access curved portions of the profile. As these parts have already been machined by the round end of the tool, the square end of the tool may skip them. When the tool encounters such a situation, each end point of the tracing edge is on a different segment. Furthermore, there will be an instance in which the leading and trailing points cannot advance further and the tool orientation cannot be solved. When this occurs, the tool continues onto the segment where the leading point lies. Fig. 13a shows a case where the round end of the tool can access the feature, but not the square end (Fig. 13b).

5 Application example

The concepts and algorithms developed in this work are illustrated in this section through their application to machining a simple star-shaped cavity (Fig. 14) on a 4-axis ram EDM. The profile was automatically classified as Type 1 by considering the lower order segments that constitute the profile and the connectivity between segment pairs, which indicated it to be G^1 continuous. A tool of type 1 was therefore found appropriate for the machining of this cavity.

Identification of tool type was followed by the calculation of the maximum permissible tool size. For profiles of type 1, only the MAT is required for calculating tool width W (see Section 3.1). The minimum value in the radius function was found to be 5 mm (Fig. 15). Accordingly, tool length calculations were based on $W = 10$ mm. From the MAT, the MIC was used to determine the tool center line length to be 34.60 mm. As the profile offset in this case comprises convex regions, tool center line lengths along these regions were also calculated as outlined in Section 3.2 (Fig. 8a), which returned a value of 36.66 mm. Fig. 15 shows the tool profiles corresponding to the MIC (A) and the convex regions of the profile (B). The minimum of these two values pertains to the maximum permissible tool length of $L = 44.60$ mm per eqn. 1. As compared to a cylindrical tool of diameter 10 mm that would be used to ED-mill this profile, the oblong tool corresponds roughly to a 430% increase in the frontal area, which is significant in terms of enhanced machining performance. With a view to demonstrating the flexibility of the proposed approach and minimizing the extent of overlapping tool paths, a shorter tool of length 25 mm was selected for the actual machining, which still provides a $\sim$300% increase in frontal area over an equivalent cylindrical tool.

On determining the tool size, the profile was offset by a distance equal to the tool length (44.6 mm) to check that there were no closed loops with offsets facing inward, which indicated that a single pass was sufficient to complete machining over each layer. To generate the tool path, the profile was offset by a distance equal to half the tool width (5 mm). The center of the arc that comprises one of the two tool ends was then constrained to and driven along the profile offset in an anti-clockwise direction. As the tool motion progresses the tool orientation is adjusted in between critical points so as to appropriately generate the profile. Fig. 16 shows several successive positions of the tool during the course of generating part of the profile, with the arrows indicating the direction of tool motion. The tool positions shown shaded correspond to critical points (positions shown in Fig. 16(b) do not entail a critical point). The direction of tool motion is reversed after the completion of machining of each layer. The scheme above was implemented on a 4-axis CNC EDM to machine the cavity seen in Fig. 17.

6 Conclusions

This paper presented a novel tooling concept that integrates the beneficial features of electrical discharge milling and die-sinking processes. The tools are of an oblong cross-section, and entail rotation and translation to machine two-dimensional cavities. The tool types are standardized to minimize their cost of manufacture and lead time. The tool geometry enables the machining of sharp features and facilitates auxiliary jet flushing for enhanced process performance. Invoking previous work that focussed on the areal effect of EDM tooling, the process can be deemed to correspond to a higher removal rate and a lower relative electrode wear, by virtue of the maximized machining engagement.

In terms of enabling computer-aided manufacture, cavity profiles were classified into three groups according to their continuity, concavity and geometric composition, which allowed for automatic tool type selection by association. Algorithms for calculating the maximum permissible tool width and length, and a tool path planning strategy for layer-by-layer machining have been presented. A sample cavity was machined on a 4-axis ram EDM to illustrate the new process.

The emphasis in the present work was on developing the concept and computer-aided manufacturing aspects of oblong tools. Further work on this innovative technology will focus on tooling/process economics with an emphasis on quantitative comparisons of process responses, aspects of tool wear sensing/compensation, and the effect of overlapping tool paths with reference to their influence on part geometric accuracy.

Acknowledgment

This work was funded by the Natural Sciences and Engineering Research Council of Canada. Authors thank M. Held for the software application that was used to compute medial axis transforms.

References

[1] G.N. Levy, B. Ferroni, Planetary spark erosion application and optimization, 16th Machine Tool Design and Research Conference, Manchester, 1976, 291–297.

[2] F. Staelens, J.P. Kruth, A computer integrated machining strategy for planetary EDM, CIRP Annals 38 (1989) 187–190.

[3] K. Saito, T. Kishinami, H. Konno, M. Sato, Development of numerical contouring control electric discharge machining, CIRP Annals 35 (1986) 117–120.

[4] M. Bayramoglu, A.W. Duffill, Systematic investigation on the use of cylindrical tools for the production of 3D complex shapes on CNC EDM machines, International Journal of Machine Tools and Manufacture 34 (1994) 327–339.

[5] M. Bayramoglu, A.W. Duffill, CNC EDM of linear and circular contours using plate tools, Journal of Materials Processing Technology 148 (2004) 196–203.

[6] S. Ding, R. Yuan, Z. Li, K. Wang, CNC electrical discharge rough machining of turbine blades, Journal of Engineering Manufacture 220 (2006) 1027–1034.

[7] P. Bleys, J.P. Kruth, Real-time tool wear compensation in milling EDM, CIRP Annals 51 (2002) 157–160.

[8] Z.Y. Yu, T. Masuzawa, M. Fujino, Micro-EDM for three-dimensional cavities: Development of uniform wear method, CIRP Annals 47 (1998) 169–172.

[9] K.P. Rajurkar, Z.Y. Yu, 3D micro-EDM using CAD/CAM, CIRP Annals 49 (2000) 127–130.

[10] Y. Ziada, P. Koshy, Rotating curvilinear tools for EDM of polygonal shapes with sharp corners, CIRP Annals 56 (2007) 221–224.

[11] M.L. Jeswani, Effect of machining area and pulse parameters on EDM performance, Indian Journal of Technology 18 (1980) 354–356.

[12] O. Blatnik, J. Valentincic, M. Junkar, Percentage of harmful discharges for surface current density monitoring in electrical discharge machining process, Journal of Engineering Manufacture 221 (2007) 1677–1684.

[13] W. Konig, L. Jorres, U. Behmer, The kinematics of planetary erosion as a basis for electro-discharge polishing and process optimization strategies, Advanced Manufacturing Processes 2 (1987) 23–35.

[14] H. Blum, A transformation for extracting new descriptors of shape, MIT Press, 1967.

[15] H. Blum, R. Nagel, Shape description using weighted symmetric axis features, Pattern Recognition 10 (1978) 167–180.

[16] M. Ramanathan, B. Gurumoorthy, Constructing medial axis transform of planar domains with curved boundaries, Computer-Aided Design 35 (2002) 619–632.

[17] E. Remy, E. Thiel, Exact medial axis with euclidian distance, Image and Vision Computing 23 (2005) 167–175.

[18] M. Held, VRONI: An engineering approach to the reliable and efficient computation of Voronoi diagrams and line segments, Computational Geometry 18 (2001) 95–123.

[19] A. Hatna, R.J. Grieve, P. Broomhead, Automatic CNC milling of pockets: geometric and technological issues, Computer Integrated Manufacturing Systems 11 (1998) 309–330.

[20] K. Tang, M. Wang, L. Chen, S. Chou, T. Woo, R. Janardane, Computing planar swept polygons under translation, Computer-Aided Design 29 (1997) 825–836.

[21] K. Sambandan, K. Kedem, K.K. Wang, Generalized planar sweeping of polygons, Journal of Manufacturing Systems 11 (1992) 246–257.

[22] Z. Ling, T.R. Chase, Generating the swept area of a body undergoing planar motion, Journal of Mechanical Design 118 (1996) 186–192.

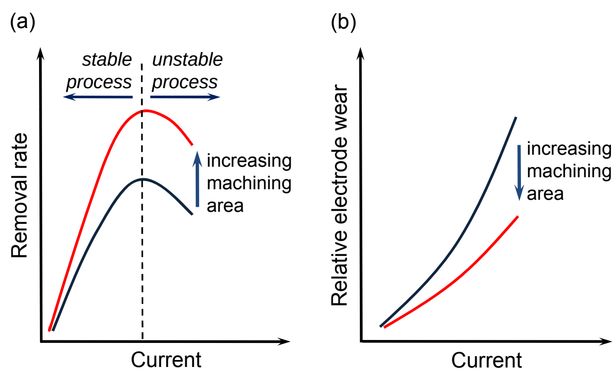

Fig. 1. Effect of apparent current density on: (a) removal rate [12], and (b) relative electrode wear [5].

1

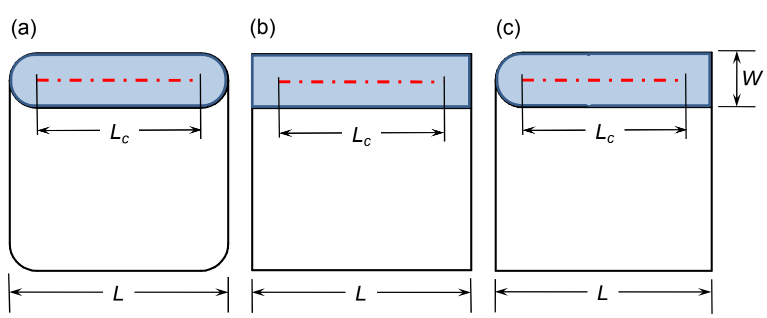

Fig. 2. Classification of profiles/tools: (a) Type 1 with round features, (b) Type 2 with sharp features, and (c) Type 3 with both round and sharp features.

2

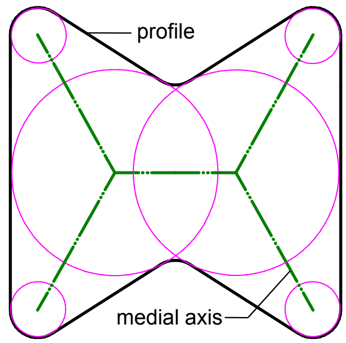

Fig. 3. Medial axis transform of a two-dimensional profile.

3

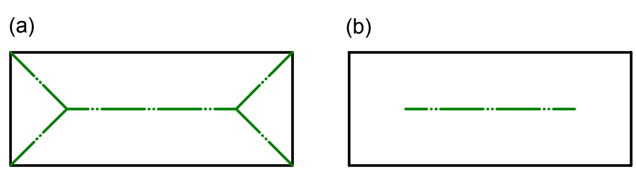

Fig. 4. (a) Medial axis, and (b) modified medial axis.

4

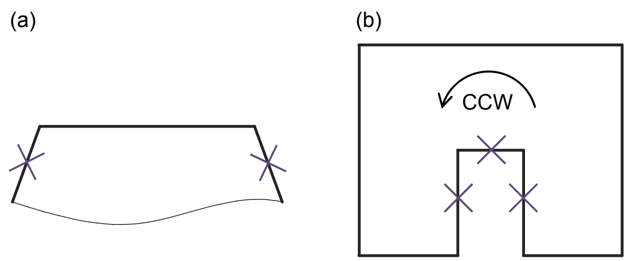

Fig. 5. Elimination of lines in Type 2 profiles with: (a) tapered, and (b) convex regions (segments denoted with a cross are discarded).

5

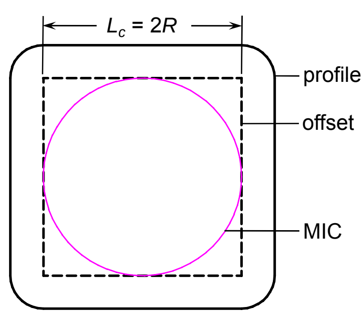

Fig. 6. Maximum inscribed circle approach to calculating tool center line length L_c.

6

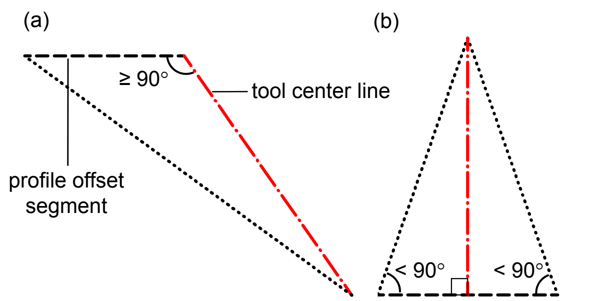

Fig. 7. Bounded region for interior angle: (a) ≥90°, and (b) <90°.

7

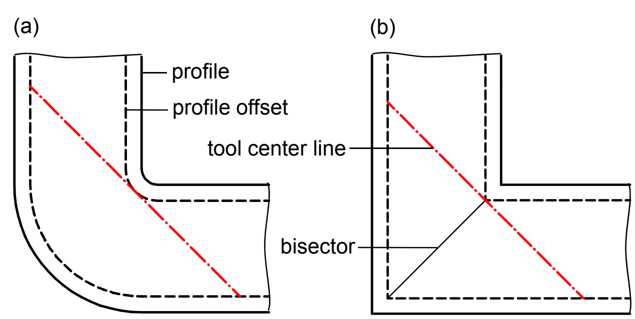

Fig. 8. Tool center line length calculation for convex regions that are: (a) G^1 continuous, and (b) G^0 continuous.

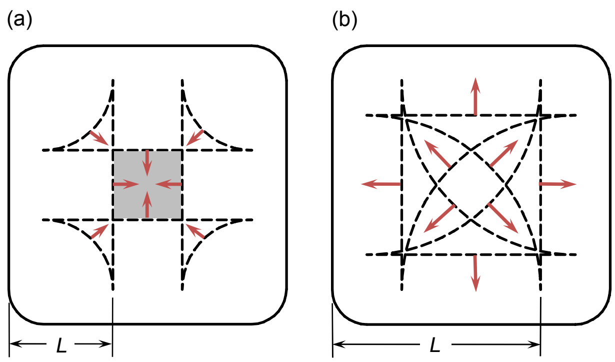

Fig. 9. Determination of the number of passes per layer.

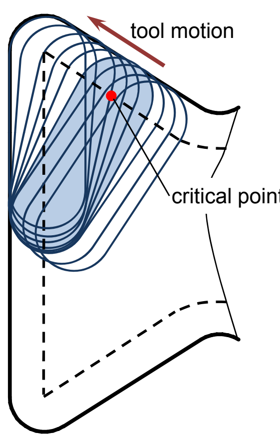

Fig. 10. Tool path planning for Type 1 profiles.

10

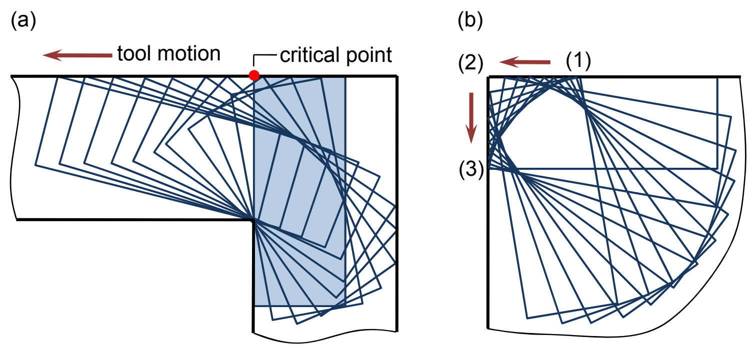

Fig. 11. Tool path planning for Type 2 profiles.

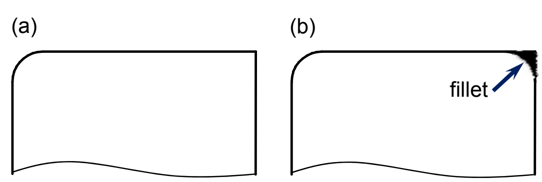

Fig. 12. Representation of Type 3 profiles.

12

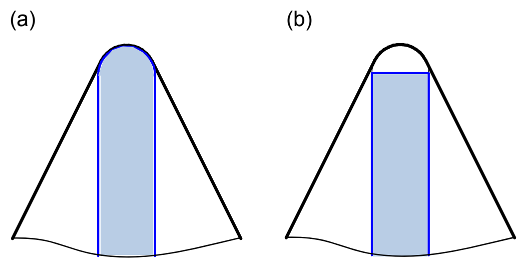

Fig. 13. Accessibility of Type 3 tools.

13

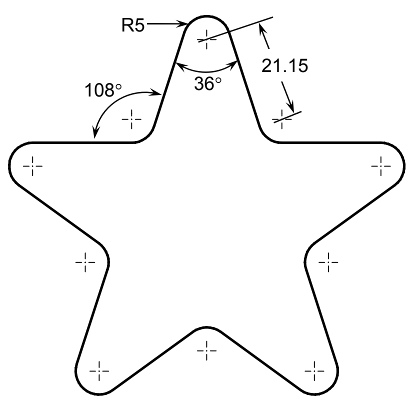

Fig. 14. Sample star-shaped cavity (dimensions in mm).

14

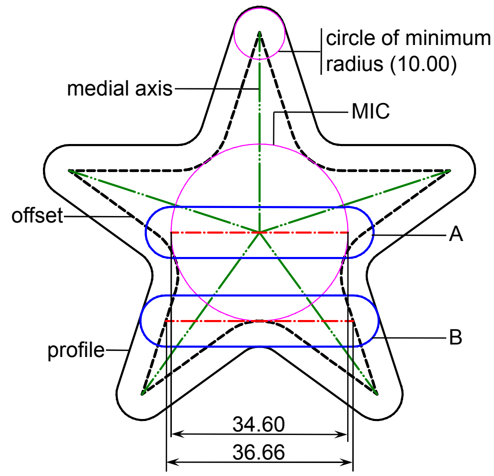

Fig. 15. Calculation of tool size (dimensions in mm).

15

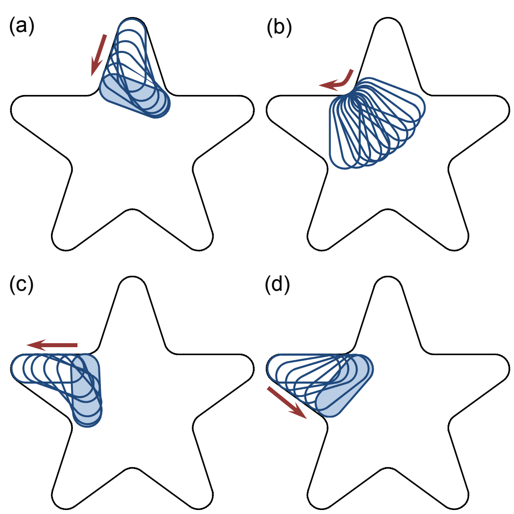

Fig. 16. Tool path for machining star-shaped cavity.

Fig. 17. Photograph of machined profile.

17

Table 1. Comparison of tool configurations.

Criterion	3D	cylindrical	oblong
Large frontal area	yes	no	yes
Good flushing	no	yes	yes
Low cost & lead time	no	yes	yes
Machine sharp corners	yes	no	yes

18